ELectronics EXpress

IEICE Electronics Express, Vol.9, No.1, 16–22

Wireless on-chip microparticle manipulation using pulse-driven dielectrophoresis

Shun Ueda[a)], **Yusuke Miyawaki, Jun Wang, Toshimasa Matsuoka, and Kenji Taniguchi**

Department of Electrical, Electronic and Information Engineering, Osaka University, 2–1 Yamada-oka, Suita, Osaka 565–0871, Japan

a) *ueda@si.eei.eng.osaka-u.ac.jp*

Abstract: A chip with which to manipulate microparticles using wireless power transfer and pulse-driven dielectrophoresis has been designed and fabricated using a 0.18-μm CMOS process. The chip enables microparticle manipulation under a 0.7-V power supply and a 13-MHz clock, which are generated on the chip by means of an on-chip coil, a rectifier, and a Schmitt trigger circuit.

Keywords: dielectrophoresis, microparticle manipulation, CMOS, wireless power transfer

Classification: Micro- or nano-electromechanical systems

References

[1] T. Hasebe, Y. Yazawa, T. Tase, M. Kamahori, K. Watanabe, and T. Oonishi, "Photosensing Resolution of Wireless Communication Chip in Inhomogeneous RF-Magnetic Field," *Jpn. J. Appl. Phys.*, vol. 45, no. 4B, pp. 3794–3798, April 2006.

[2] Y. Ghallab and W. Badawy, "Sensing Methods for Dielectrophoresis Phenomenon: From Bulky Instruments to Lab-on-a-Chip," *IEEE Circuits Syst. Mag.*, vol. 4, no. 3, pp. 5–15, 2004.

[3] S. Tsukahara, T. Sakamoto, and H. Watarai, "Positive Dielectrophoretic Mobilities of Single Microparticles Enhanced by the Dynamic Diffusion Cloud of Ions," *Langmuir*, vol. 16, no. 8, pp. 3866–3872, April 2000.

[4] Y. Huang and R. Pethig, "Electrode design for negative dielectrophoresis," *Meas. Sci. Technol.*, vol. 2, no. 12, pp. 1142–1146, Dec. 1991.

[5] T. Fujita, Y. Kaneko, and S. Abe, "Contactless Power Transfer System using Series and Parallel Resonant Capacitors," *IEEJ Trans. Industry Applications*, vol. 127, no. 2, pp. 174–180, Feb. 2007 (in Japanese).

[6] T. Matsuoka, J. Wang, T. Kihara, H. Ham, and K. Taniguchi, "Low-Voltage Wireless Analog CMOS Circuits toward 0.5 V Operation," *IEICE Trans. Fundamentals*, vol. E93-A, no. 2, pp. 356–366, Feb. 2010.

[7] C. Zhang, A. Srivastava, and P. K. Ajmera, "Low voltage CMOS Schmitt trigger circuits," *Electron. Lett.*, vol. 39, no. 24, pp. 1696–1698, Nov. 2003.

[8] K. Kotani, A. Sasaki, and T. Ito, "High-Efficiency Differential-Drive CMOS Rectifier for UHF RFIDs," *IEEE J. Solid-State Circuits*, vol. 44, no. 11, pp. 3011–3018, Nov. 2009.

DOI: 10.1587/elex.9.16
Received October 28, 2011
Accepted December 02, 2011
Published January 10, 2012

[9] K. Niitsu, Y. Yuxiang, H. Ishikuro, and T. Kuroda, "A 33% Improvement in Efficiency of Wireless Inter-Chip Power Delivery by Thin Film Magnetic Material for Three-Dimensional System Integration," *Jpn. J. Appl. Phys.*, vol. 48, no. 4, p. 04C073-1, April 2009.

1 Introduction

In recent years, sensor and control circuits have been integrated on chips in order to realize more compact, inexpensive, and easy-to-use equipment. Wireless power transfer can improve these features [1]. In addition, manipulation of particles and cells is also useful for efficient sensing. Dielectrophoresis (DEP), in which particles move under the influence of a driving force generated by the gradient of the electric field intensity [2, 3], is a promising technique for this purpose.

The DEP force $< F_{DEP} >$ acting on particles of radius r_e in a liquid medium with permittivity ϵ_m is given by the following equations [2]:

$$< F_{DEP} > = 2\pi r_e^3 \epsilon_m Re[\underline{Ke}] \nabla E_{rms}^2, \quad (1)$$

$$\underline{Ke} = \frac{\underline{\epsilon_p} - \underline{\epsilon_m}}{\underline{\epsilon_p} + 2\underline{\epsilon_m}}, \quad (2)$$

where E_{rms} is the applied local RMS electric field, and $\underline{\epsilon_m}$ and $\underline{\epsilon_p}$ are the complex permittivities of the liquid medium and the particle, respectively, where the conductive loss is considered. The real part of the Clausius-Mossotti factor $\underline{Ke}$ determines the direction of the DEP force. When the direction of the DEP force is positive (negative), particles are attracted to the electric field intensity maxima (minima) and are repelled from the minima (maxima) by the positive (negative) DEP. The particle migration is determined by the balance between the DEP and frictional forces [3]. In the case of negative DEP, a quadrupole electrode structure [3, 4] is used to easily capture particles near the center of the working area.

In the present letter, on-chip DEP microparticle manipulation has been demonstrated without electrical wires. In order to realize a compact low-power driving circuit using a CMOS digital circuit, pulse-driven DEP is used in place of conventional sinusoidal DEP. The proposed technique enhances usability in microparticle manipulation, and may enable new fabrication technologies involving small particles.

2 Pulse-driven dielectrophoresis

In order to evaluate the particle motion of pulse-driven DEP, experiments using polystyrene particles (diameter: 10 μm) in $NaHCO_3$ aqueous solution (conductivity: $\sigma_m = 60$ mS/m) were carried out at room temperature. Here, copper quadrupole electrodes (thickness: 20 μm, width: 200 μm, diagonal inter-electrode space: 300 μm) were used on a glass board. After dropping the $NaHCO_3$ aqueous suspensions containing the polystyrene particles onto the

DOI: 10.1587/elex.9.16
Received October 28, 2011
Accepted December 02, 2011
Published January 10, 2012

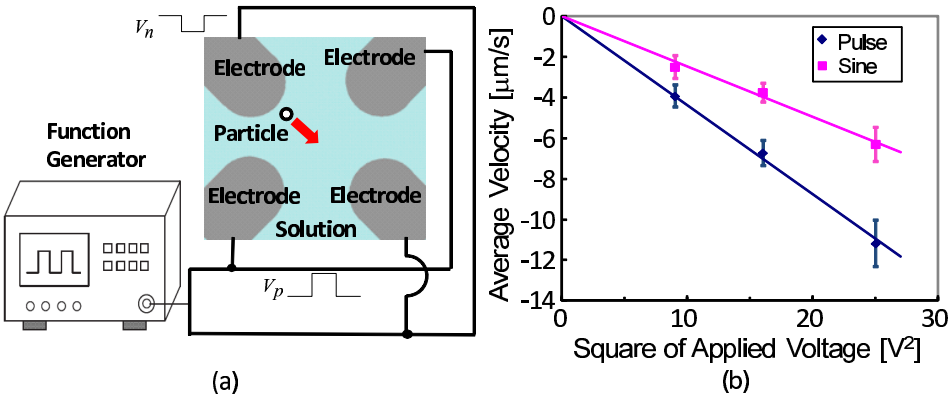

Fig. 1. (a) Experimental setup of pulse-driven DEP, (b) dependence of average velocity of polystyrene microparticle by DEP ($r_e = 5\,\mu$m, $\sigma_m = 60\,$mS/m) on applied voltage amplitude (frequency: 1 MHz).

DEP working area, the driving signals (frequency: 1 MHz) are applied to the electrodes, where electrodes located at opposite corners have the same signal polarity, as shown in Fig. 1 (a). The average velocities of the microparticles were obtained based on microscope observations of the position changes of the particles caused by DEP driving.

Figure 1 (b) shows the dependence of the average velocity of the particles on the applied voltage amplitude. $< F_{DEP} >$ is proportional to the square of the applied voltage. The velocity enhancement by a factor of 1.7 in the pulse-driven DEP, as compared to the sinusoidal DEP, corresponds to the squared ratio between fundamental components in the Fourier series expansion of the 50%-duty pulse signal and a sinusoidal signal for the same amplitude conditions, i.e., $(4/\pi)^2$. Thus, the pulse-driven DEP is useful for faster microparticle manipulation, as well as the realization of a digital DEP driving circuit.

3 Chip design

In order to enhance usability in microparticle manipulation by eliminating electrical connections to external equipment, sufficient power for on-chip DEP operation is delivered through wireless power transfer using a primary series and secondary parallel resonant capacitors [5], as shown in Fig. 2 (a). From the sinusoidal AC signal received by the on-chip secondary coil coupled inductively with an external primary coil, the on-chip DC supply V_{DD} and the clock signal are generated using the rectifier and the Schmitt trigger circuits, respectively. The frequency divider generates the DEP driving signal.

In order to prevent the solution temperature from increasing due to the power consumption of the chip and wireless power transfer loss through the chip, the chip must operate at a low supply voltage for low delivered power and low consumption power. Therefore, we set on-chip supply voltage to $V_{DD} = 0.7\,$V and the frequency of the wireless power transfer to 13 MHz. The chip is designed using a 0.18-μm CMOS process and implements forward

DOI: 10.1587/elex.9.16
Received October 28, 2011
Accepted December 02, 2011
Published January 10, 2012

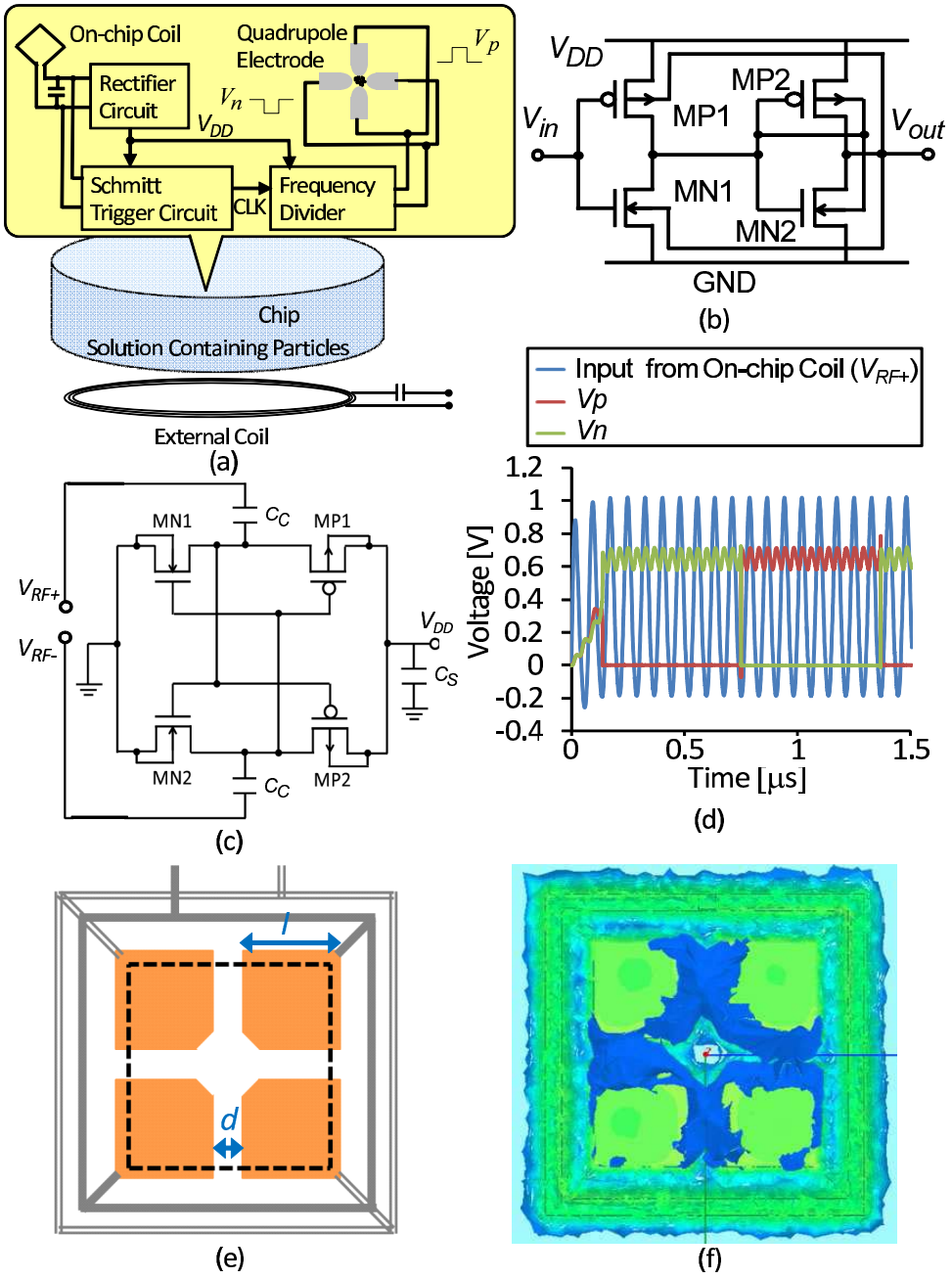

Fig. 2. (a) Configuration and operating environment of the chip, (b) Schmitt trigger circuit, (c) CMOS rectifier circuit, (d) simulation results for the circuit part of the chip at the RF sinusoidal input from the secondary on-chip coil (amplitude: 1.2 V, frequency: 13 MHz), (e) layout of quadrupole electrodes and their interconnects with an open working area designated by dashed lines (electrode widths: $l\,[\mu\mathrm{m}]$, spaces between adjacent electrodes: $d\,[\mu\mathrm{m}]$), and (f) electromagnetic simulation results for the electrode structure obtained using Ansoft HFSS.

DOI: 10.1587/elex.9.16
Received October 28, 2011
Accepted December 02, 2011
Published January 10, 2012

body biasing for low voltage operation [6].

3.1 Circuit design

The Schmitt trigger circuit shown in Fig. 2 (b) [7] shows the hysteresis with the forward-body biasing in MN1 and MP1 according to the output voltage. In the second stage, a dynamic threshold MOS configuration is used for inverter operation at a supply voltage of less than 0.7 V. The switching voltages of the Schmitt trigger for input sweep from zero to V_{DD} and the opposite-direction sweep, i.e., V_h and V_l, are given by [7]

$$V_h = \frac{V_{DD} - |V_{thf,p}| + \sqrt{\beta_n/\beta_p}\, V_{tho,n}}{\sqrt{\beta_n/\beta_p} + 1}, \tag{3}$$

$$V_l = \frac{V_{DD} + \sqrt{\beta_n/\beta_p}\, V_{thf,n} - |V_{tho,p}|}{\sqrt{\beta_n/\beta_p} + 1}, \tag{4}$$

where β_n and β_p transconductance parameters, $V_{tho,n}$ and $V_{tho,p}$ are zero-body-bias threshold voltages, $V_{thf,n}$ and $V_{thf,p}$ are the V_{DD}-forward-body-bias threshold voltages of the nMOS and pMOS devices, respectively. The hysteresis width V_{hw} of the Schmitt trigger is given by

$$V_{hw} = V_h - V_l = \frac{|V_{tho,p}| - |V_{thf,p}| + \sqrt{\beta_n/\beta_p}\ (V_{tho,n} - V_{thf,n})}{\sqrt{\beta_n/\beta_p} + 1}. \tag{5}$$

The hysteresis width can be tuned through the size ratio of MP1 and MN1. In this design, the hysteresis width of $V_{hw} = 0.2$ V is realized under $V_{DD} = 0.7$ V by using the MN1 and MP1 gate widths of $W_n = 1\,\mu$m and $W_p = 2\,\mu$m for the minimum gate length ($0.18\,\mu$m).

In this design, the CMOS rectifier circuit shown in Fig. 2 (c) is used due to its high efficiency [8]. The rectifier has a cross-coupled differential configuration driven by a differential RF input. Through body-source biasing, both low on-resistance and small reverse leakage of the MOS transistors are realized. In the steady state, the output DC voltage is determined by a balance among forward-transferred charges, reverse-transferred charges, and charges flowing to an output load. In this design, the nMOS and pMOS gate widths for the minimum gate length are $W_n = 2\,\mu$m and $W_p = 5\,\mu$m, respectively. Capacitances of $C_c = C_s = 10$ pF are used. For a differential RF input of approximately 1.2 V amplitude and a frequency of 13 MHz, V_{DD} can be estimated to be 0.7 V.

As shown in Fig. 2 (d), the simulation results for circuit blocks verify that the on-chip supply V_{DD}, clock signal (CLK), and DEP driving pulse signals (V_p and V_n) are generated through the wireless power transfer by the rectifier circuit, the Schmitt trigger circuit, and the frequency divider with a division ratio of 16.

3.2 Quadrupole electrode structure

The quadrupole electrodes are formed with the top metal. As shown in Fig. 2 (e), each quadrupole electrode is surrounded by a ring of differential

DOI: 10.1587/elex.9.16
Received October 28, 2011
Accepted December 02, 2011
Published January 10, 2012

signal interconnects, resulting in short single-end interconnection that provides a DEP driving signal to the electrode. Such an interconnect topology can prevent undesired electric fields and consequent DEP. The electromagnetic simulation results of the quadrupole electrode structure, as shown in Fig. 2 (f), ensure that the electric field is confined to the differential signal ring and the quadrupole electrode. This feature prevents electric crosstalk between several quadrupole electrodes formed on the same chip.

4 Experimental results

A microphotograph of the test chip fabricated using a 0.18-μm CMOS process is shown in Fig. 3 (a). The chip area is 6.25 mm^2, including an on-chip, one-turn coil near the chip edge. The on-chip coil is formed with the two top metal layers in parallel to reduce resistive loss. A magnetic sheet (ALPS HM-

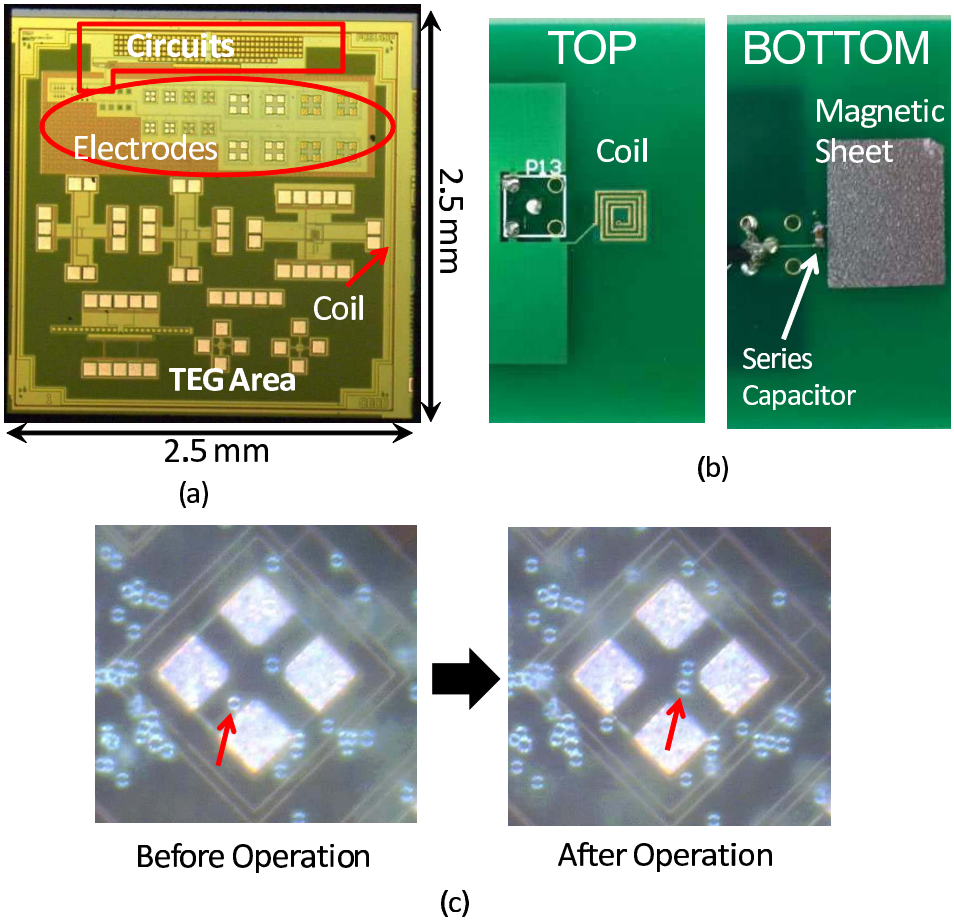

Fig. 3. (a) Optical micrograph of the fabricated chip and (b) photograph of the board for wireless power transfer. (c) Microscope observation for negative DEP of polystyrene microparticles (r_e = 5 μm) in the $NaHCO_3$ aqueous suspensions (σ_m = 60 mS/m) on the working area with (l, d) = (50, 30) where the input voltage of the external primary coil with the series capacitor is sinusoidal (amplitude: ~75 V, frequency: 13 MHz).

DOI: 10.1587/elex.9.16
Received October 28, 2011
Accepted December 02, 2011
Published January 10, 2012

SZS21020, permeability: $80 - j25$ at 13.56 MHz) embedded on the bottom side of the external primary coil, as shown in Fig. 3 (b), improves the wireless power transfer efficiency by over 30% as reported for the inter-chip case [9]. After dropping the $NaHCO_3$ aqueous suspensions ($\sigma_m = 60$ mS/m) containing the polystyrene microparticles ($r_e = 5\,\mu$m) onto the chip, AC power is provided to the chip through the wireless power transfer to apply driving signals in the quadrupole electrodes for the DEP operation.

As shown in Fig. 3 (c), microscope observation of the on-chip microparticle manipulation reveals particle motion toward center of the working area (minimum of the electric field), indicating negative DEP. On-chip microparticle manipulation without any electrical connections has been achieved.

5 Conclusion

In order to achieve easy-to-use on-chip microparticle manipulation, we have developed a chip that can manipulate microparticles by pulse-driven DEP in a solution without any electrical interconnections. The chip has an on-chip coil for wireless power transfer and 0.7-V operation circuits using forward body biasing of the MOS devices.

Although the present study is preliminary, we believe that the findings presented herein will help to enhance usability in sensing and analysis devices and facilitate the realization of a new above-CMOS fabrication solution.

Acknowledgments

The present study was supported in part by a Grant-in-Aid for Scientific Research (KAKENHI) (C) (2056324) and by the Ministry of Education, Culture, Sports, Science and Technology of Japan through a grant to the Osaka University Global COE Program, “Center for Electronic Devises Innovation”. The VLSI chip in the present study was fabricated as part of the chip fabrication program of the VLSI Design and Education Center (VDEC) at the University of Tokyo in collaboration with Rohm Co., Ltd.

DOI: 10.1587/elex.9.16
Received October 28, 2011
Accepted December 02, 2011
Published January 10, 2012